CHAPTER FIVE

SYNTHESIS AND CHARACTERISTICS STUDY OF PI/TiO_2 NANO HYBRID FILMS

Summary

The work presented here focuses on preparation of BAO-ODPA polyimide/TiO_2 nano hybrid films by sol-gel process using titanium ethoxide as an additive and polyimide as the matrix. The rate of the hydrolysis reaction of titanium alkoxide can be controlled by using acetylacetone (acac) through the formation of an acetylacetate complex. The amount of titania (TiO_2) is varied from 5.0 to 40.0 wt% under the assumption of complete conversion of titanium ethoxide to titania. The resultant BAO-ODPA/TiO_2 nano hybrid films are characterized with regard to their structure, morphology, optical, and thermal properties.

5.1 Titanium Precursor

The nano hybrid films of titania (TiO_2) in polyimide (PI) from 2,5-bis(4-amino-phenyl)1,3,4-oxadiazole (BAO) and 4,4′-oxydiphthalic anhydride (ODPA) have been successfully fabricated by an in-situ sol-gel process.

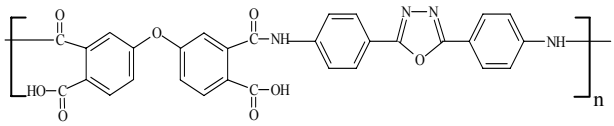

Figure 5.1 Poly(amic acid) (PAA) from BAO/ODPA.

In this study, $Ti(OEt)_4$ is used as a TiO_2 source in the hybridization system. However, when it is dropped directly into the poly(amic acid) (PAA), gelation occurred and lumps formed which can not be dispersed by vigorously stirring. That is attributed to titanium alkoxide with very high reaction activity, which

results in fast hydrolysis and strong interaction with polymer. In order to slow the hydrolysis and condensation reactions, chemical additive such as acetylacetone is used as a chelating agent to stabilize the titanium alkoxide through the formation of an acetylacetate complex. After forming a complex with the chelating ligand, the species between the metal and the chelating ligand is less easy to hydrolyze. The reaction between the titanium alkoixde and the acetylacetone is suggested in Figure 5.2. Acetylacetone exhibits keto-enol tautomerism. The enol form, containing a reactive hydroxyl group, reacts very readily with titanium alkoxide to give the structure where the enol form of the acac is stabilized by chelating with the titanium to form six-member ring [1-3].

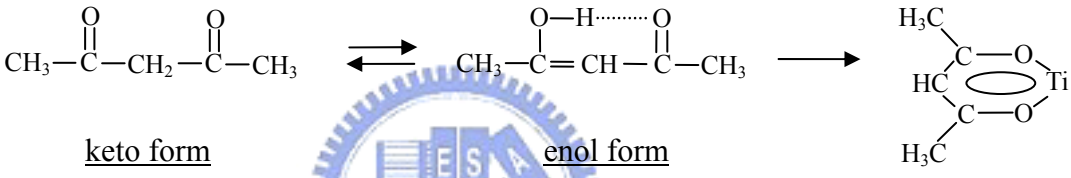

Figure 5.2 The reaction between acetylacetone and titanium alkoxide.

5.2 FT-IR Analysis

The chemical structures of pure polyimide and PI/TiO_2 hybrid films are characterized with a FT-IR spectrometer over the spectral region of 400-4000 cm^{-1}. As shown in Figure 5.3, the characteristic peaks of symmetric C=O stretching and asymmetric C=O stretching of the imide group are clearly visible at ~1720 and ~1780 cm^{-1}, respectively. The assignment of the stretching of the imide ring is at 1380 cm^{-1} [4]. The above mentioned peaks are the characteristic absorption of imide group and are shown in the spectra of the entire pure polyimide and PI/TiO_2 hybrid films. The introduction of the TiO_2 leads to a broad and strong absorption band from approximately 850 to 400 cm^{-1} [5-6]. According to Figure 5.3, this region gradually increases in intensity with increasing TiO_2 content. Moreover, it

is observed that the intensity of a broad OH stretching from 3100-3500 cm^{-1} becomes stronger with increasing the TiO_2 content. This is probably a result of the Ti-OH residue groups in the TiO_2 domains [7-8].

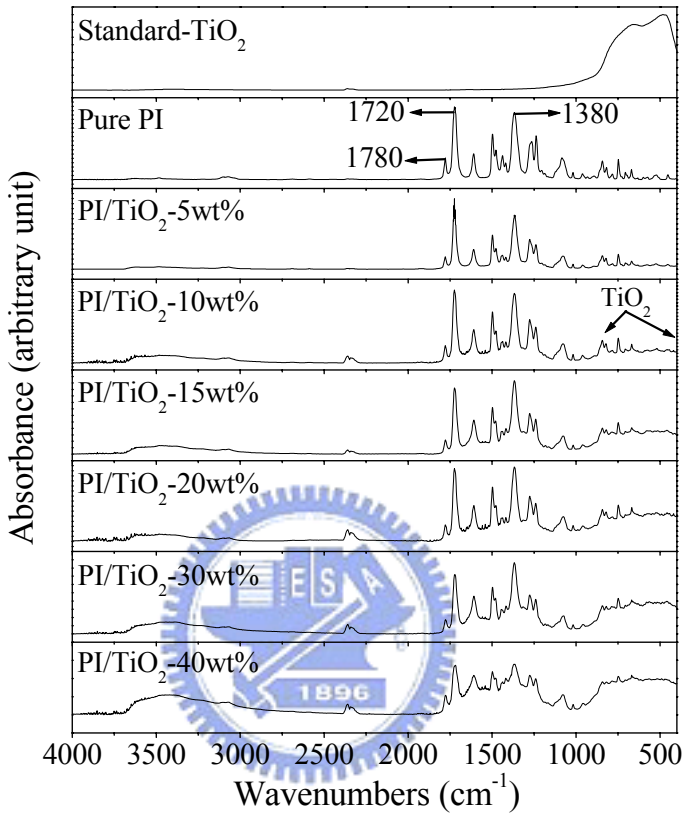

Figure 5.3 FT-IR absorption spectra of the PI/TiO_2 hybrid films.

5.3 UV-vis Transmittance Analysis

An Agilent 8452 UV/VIS spectrometer is used to examine UV-visible transmission spectra of the PI/TiO_2 hybrid films coated on quartz glass in the range of 200-1100 nm. Figure 5.4 shows the optical transmittance spectra of the hybrid films with different TiO_2 contents. It can be seen that the transmittance of the hybrid films becomes lower as the TiO_2 content increases. For pure polyimide and PI/TiO_2-5 wt% hybrid film, little absorption can be observed at 330 nm or longer wavelengths. Whereas, as the weight percentage of TiO_2 is increased more than 10,

a relatively strong absorption up to the wavelength of 400 nm can be clearly seen. It is suggested that the decrease in transmittance with the increase of TiO_2 content may be resulted from a complex formed during the preparation of Ti precursor.

In this study, titanium ethoxide is used as a TiO_2 source in the sol-gel reaction. Nevertheless, this alkoxide is not used directly because its high hydrolysis rate could result in gelation. As a result, acetylacetone is employed to reduce the reaction rate through the formation of an acetylacetate complex. However, this complex has been proven to have a strong absorption band in the visible region [9]. The effect of the complex is more evident with increasing TiO_2 content, hence produces a stronger absorption in the visible region. Another interesting observation from Figure 5.4 is the drastically increase of the absorption between 5 wt% and 10 wt%. This result may be attributed to the aggregation of metal oxide, thereby causes growth of particle size and leads to large scattering [10].

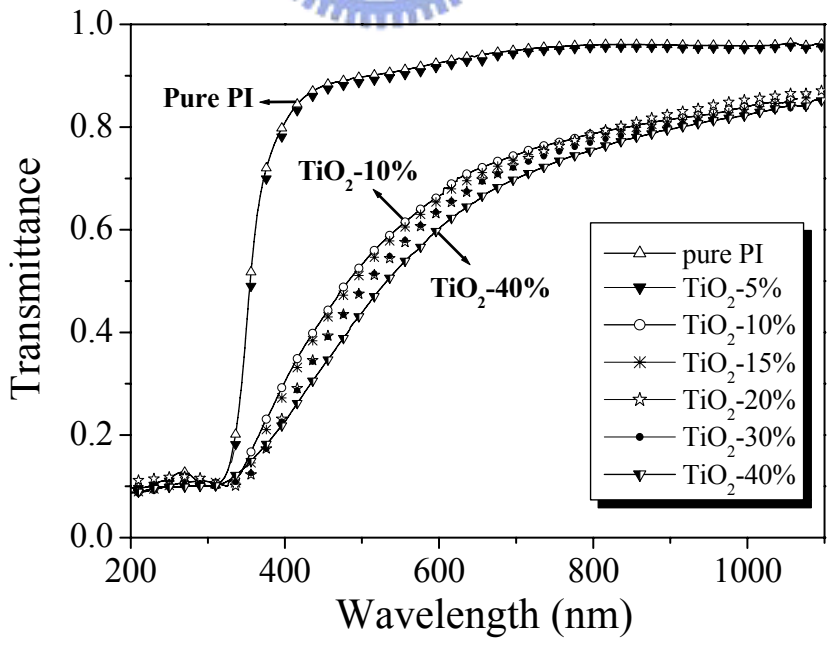

Figure 5.4 UV-visible spectra of the PI/TiO_2 hybrid films.

5.4 XRD Analysis

The XRD patterns of the PI/TiO_2 hybrid films, pure polyimide, and standard of TiO_2 (anatase) powder are shown in Figure 5.5. Pure polyimide film and the standard of TiO_2 (anatase) powder both display crystalline structures [11-15]. The main diffraction peaks for pure polyimide are found at 2θ = 15.7°, 22.1°, and 24.8° corresponding to d-spaces of 5.65, 4.01, and 3.58Å, respectively. On the other hand, the XRD patterns of PI/TiO_2 hybrid films only reveal essentially an amorphous hump centered at 24° that originated from amorphous phase of aromatic polyimide. None of the typical crystalline peaks, associated with the TiO_2 and polyimide structures can be seen. This result indicates that pure polyimide has some intermolecular regularity during the film fabrication process and the introduction of TiO_2 disrupts this crystallinity in the hybrid films.

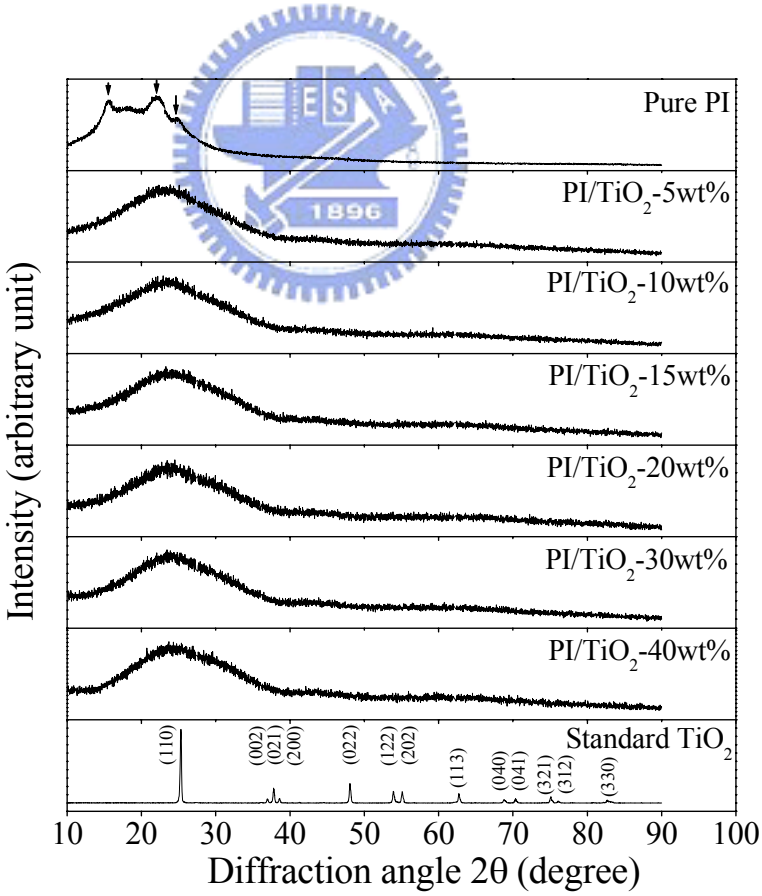

Figure 5.5 XRD patterns of pure PI, PI/TiO_2 hybrid films and standard of TiO_2 (anatae).

5.5 XPS Analysis

XPS spectra of PI/TiO_2 hybrid films are shown in Figure 5.6 to 5.8. The surface chemical composition of PI/TiO_2-40 wt% hybrid film, determined from the survey spectrum of Figure 5.6, consists of carbon, oxygen, nitrogen, and titanium.

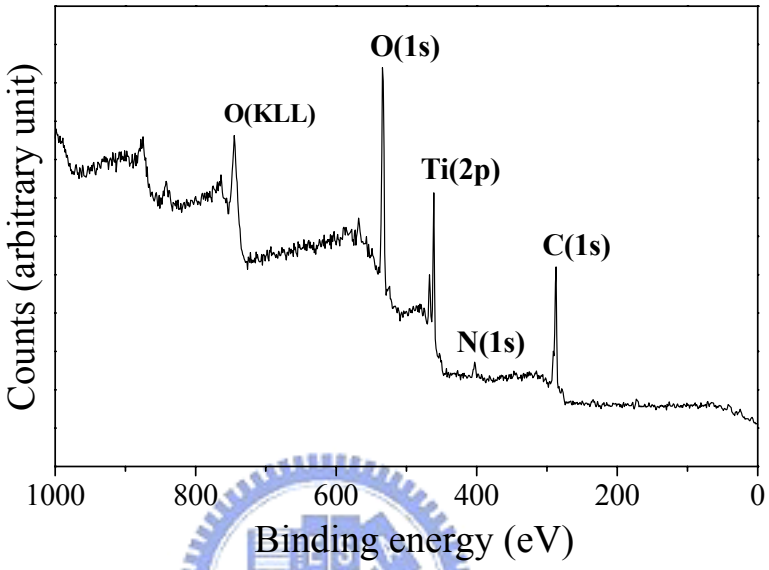

Figure 5.6 XPS survey spectrum of the PI/TiO_2 -40 wt% hybrid film.

Figure 5.7 shows the composition-depth profiles for the titanium component in the PI/TiO_2-30 wt% hybrid film. The binding energies of TiO_2 can be observed at 459.5 and 465.4 eV for Ti $2p_{3/2}$ and Ti $2p_{1/2}$, respectively [16-18]. Figure 5.7 demonstrates that longer sputtering time results in an increase in the intensity of titanium species. It is implied that the concentration of the titanium species increase on going from the surface to the bulk. This result is in contrary to the previous reports which the migration of the dopant species from the bulk to the surface of the polymer is often observed [19]. According to the concept of "site isolation" [20], metal alkoxides is maintained in isolated pockets in the polymeric matrix and this can be achieved by pre-binding the metal alkoxide precursor to the carboxylic sites of the poly(amic acid). Besides, the rigidity of polyimide

backbone and the network structure of TiO_2 not only slow the mobility of the titanium alkoxide, but also impede the migration of titanium to the hybrid film surface (oxygen-rich). Both the reasons may be resolved why smaller amount of titanium atom is noticed on the hybrid film surface.

Furthermore, the shift in the Ti 2p binding energy is a result of the titanium atom in different chemical environment. The presence of the molecular oxygen in the air-side is a probable explanation for why the titanium atoms on the surface have higher binding energy, whereas the titanium atoms in the bulk have lower binding energy. Due to the lack of molecular oxygen in the bulk, the conversion of titanium alkoxide to TiO_2 is not complete. Conversely, it can be said that there is more amount of oxygen contained in the air-side, the conversion of titanium alkoxide to TiO_2 is more extensively.

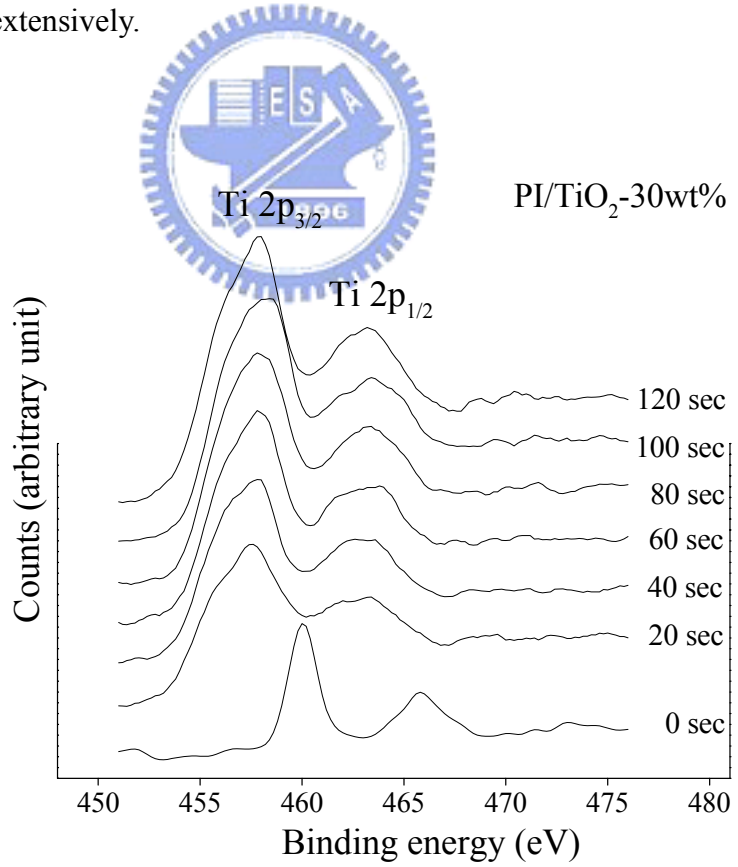

Figure 5.7 The composition-depth profiles for the titanium component in the PI/TiO_2-30 wt% hybrid film.

Figure 5.8 indicates the intensity of Ti 2p increases with increasing the content of TiO_2. Here, the slight shift in the Ti 2p binding energy is attributed to the same reason mentioned before. Due to the more amounts of titanium atoms incorporated in the hybrid films, therefore, the more diverse compounds are formed and resulted in the small shift of Ti 2p peaks. XPS reveals quantitative information of surface composition (≤50 Å) of the hybrid films. The molar percent is calculated under an assumption that all the titanium ethoxide converted to TiO_2. Table 5.1 lists the surface content of Ti for the hybrid films measured by XPS. It can be seen that the molar percentages of experimental values are much less as compared with the theoretical Ti content. In addition, the ratio, experiment value to theoretical value, increases with increasing the TiO_2 content up to 20 wt% and it reaches a constant as TiO_2 content over 20 wt%. Apparently, the amount of Ti on the hybrid film surface is lower than that in the bulk. This result is consistent with the statement of Figure 5.7.

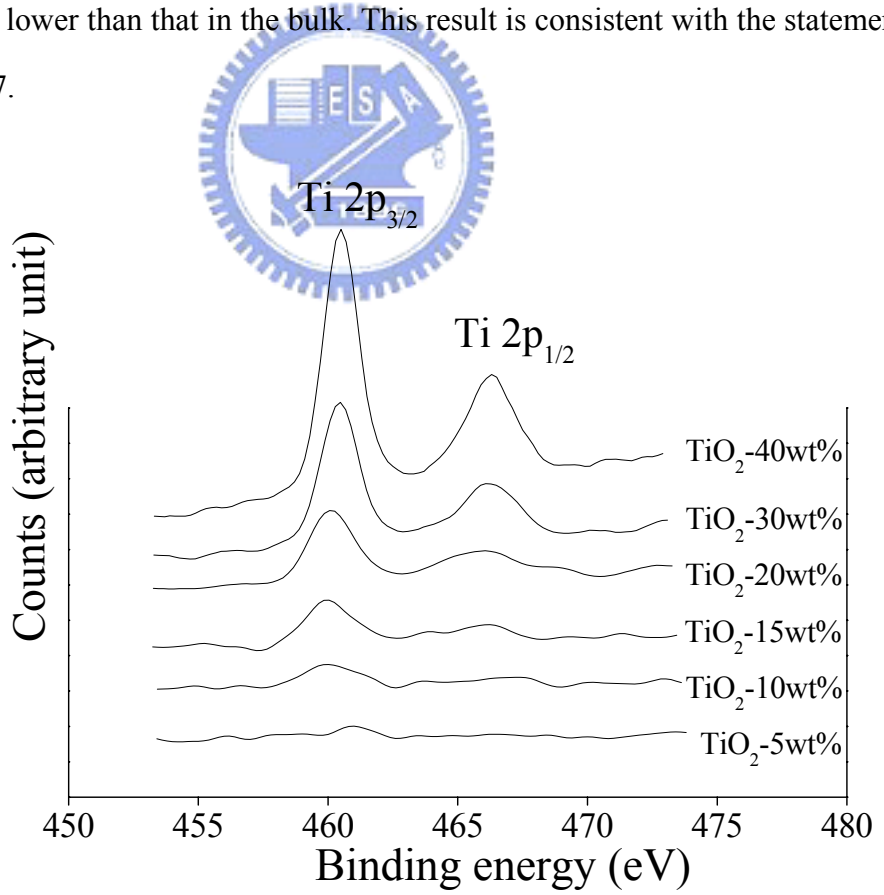

Figure 5.8 XPS spectra of Ti 2p in hybrid films.

Table 5.1 The surface content of Ti atoms for PI/TiO_2 hybrid films measured by XPS.

Sample	Experimental value Ti (mol %)	Theoretical value Ti (mol %)	Experimental value / Theoretical value
PI/TiO_2-5 wt%	0.13	0.86	0.15
PI/TiO_2-10 wt%	0.53	1.80	0.29
PI/TiO_2-15 wt%	0.92	2.83	0.33
PI/TiO_2-20 wt%	1.38	3.95	0.35
PI/TiO_2-30 wt%	3.17	6.60	0.34
PI/TiO_2-40 wt%	3.37	9.90	0.34

5.6 TEM Analysis

To probe the internal structure of the hybrid films, ultramicrotomed cross sections of the PI/TiO_2 hybrid films are examined by TEM. The TEM images in different magnification are shown in Figures 5.9 and 5.10. In the case of PI/TiO_2-5 wt%, the spherical shape nano particle with a diameter of 10 nm is observed. In the other case of PI/TiO_2 hybrid film, up to a TiO_2 content of 30 wt%, reveals a uniform distribution of spherically shaped particles, 40 nm in size, throughout the bulk of the hybrid film. The spatial distribution of PI/TiO_2-30 wt% hybrid film is denser as compared with the PI/TiO_2-5 wt% one. Besides, the particle size is dependent upon the TiO_2 content in the hybrid films. Figure 5.11 (a) and (b) are the selected-area electron diffraction (SAED) patterns of the dark area in Figures 5.9 and 5.10. This analysis further confirms the results of XRD and indicates the diffraction facets of the TiO_2 phase, meaning (200), (112), (040), (400) and (351), respectively.

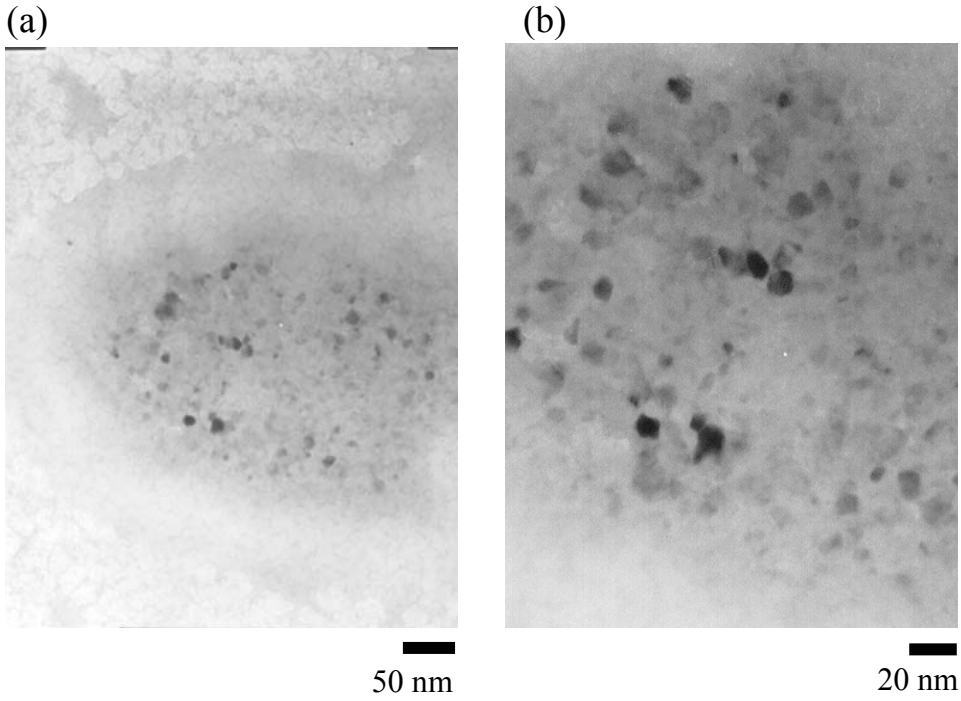

Figure 5.9 TEM photographs of the PI/TiO_2-5 wt% hybrid film in different magnification.

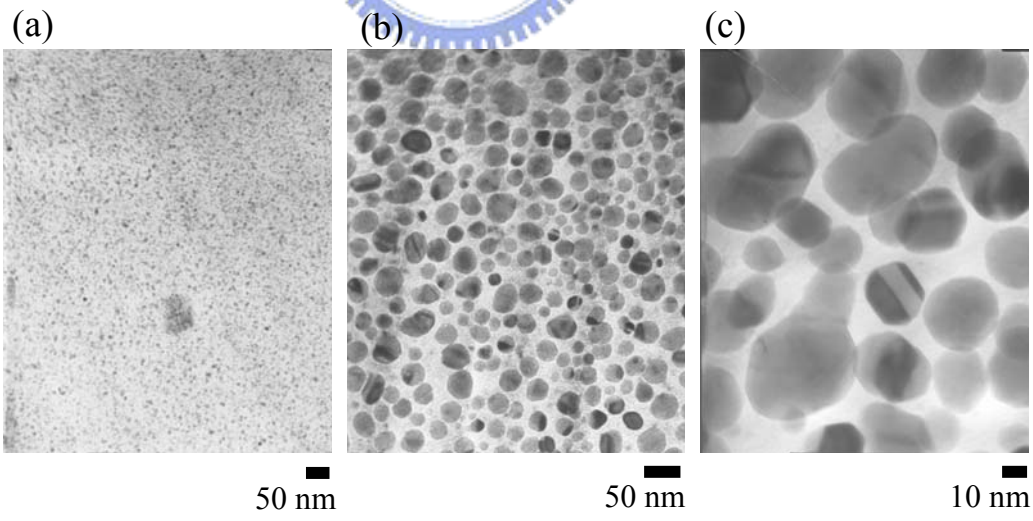

Figure 5.10 TEM photographs of the PI/TiO_2-30 wt% hybrid film in different magnification.

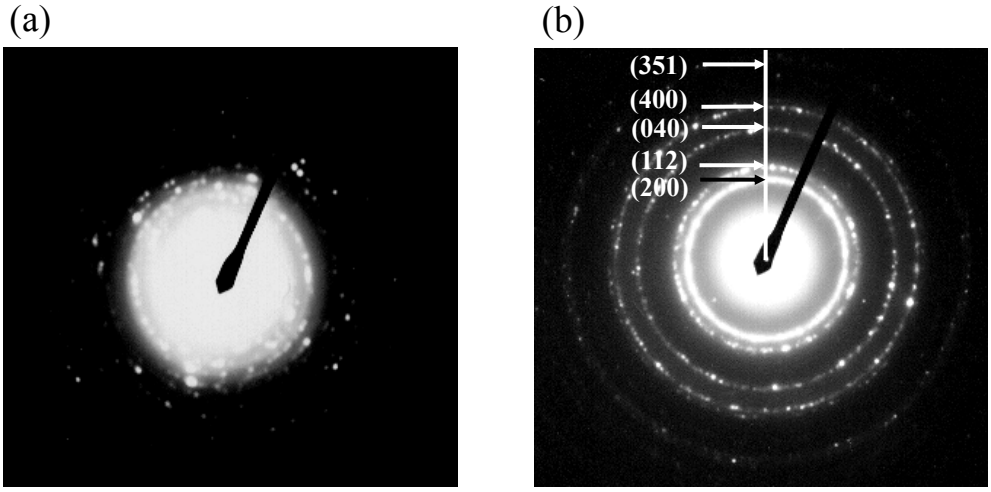

Figure 5.11 Selected-area electron diffraction (SAED) patterns (a) PI/TiO_2-5 wt% (b) PI/TiO_2-30 wt%.

5.7 Thermal Decomposition Analysis

Figure 5.12 shows the thermal gravimetric profiles of the PI/TiO_2 hybrid films. The thermal stabilities of all the hybrid films are inferior to that of pure polyimide. The introduction of TiO_2 causes a slight decrease (40℃) in thermal stability of hybrid films. Boggess and Taylor have pointed out that metallic compounds can oxdatively degrade polyimide films [21-22]. These considerable decreases in thermal stability may be related to metal-catalyzed oxidative decomposition in the hybrid films. It also can be seen that the weight residue remaining at 800℃ is proportional to the content of TiO_2 incorporated. The thermal resistance of the PI/TiO_2 hybrid films is reduced by incorporation of TiO_2; however, they are still good for practical applications.

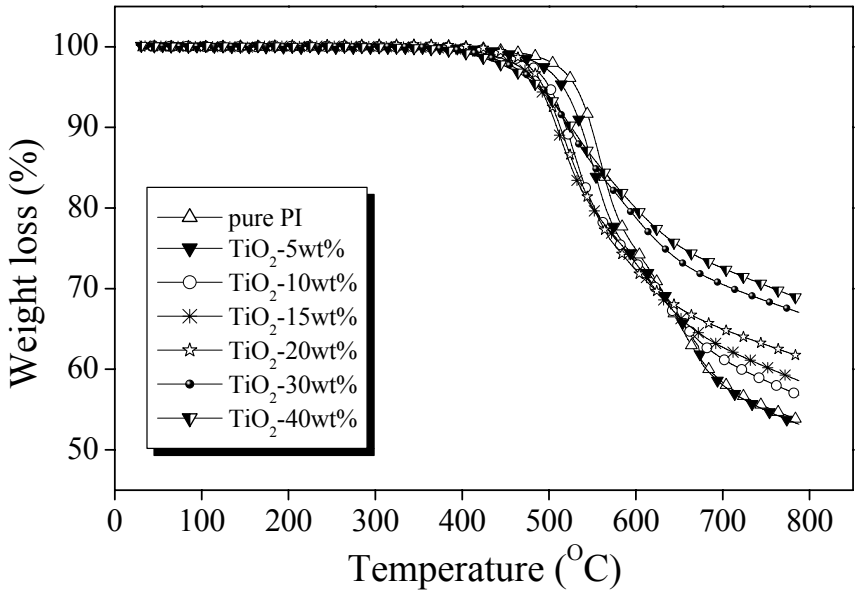

Figure 5.12 Thermogravimetric profiles of the PI/TiO_2 hybrid films.

5.8 Conclusion

The PI/TiO_2 nano hybrid films have been successfully fabricated by sol-gel process. The new PI/TiO_2 hybrid films have fair good optical transparency and thermal stability, even with TiO_2 content up to 40 wt%. According to the TEM analysis, nanocrystallines of TiO_2 with diameters of 10 and 40 nm are well-dispersed in the polyimide matrix for the PI/TiO_2-5 wt% and PI/TiO_2-30 wt% hybrid films, respectively. Nevertheless, the introduction of TiO_2 disrupts the intermolecular regularity of polyimide chains. The composition-depth profiles of the hybrid films show that the titanium atoms on the topmost surface are lower than that in the bulk. With increasing the TiO_2 up to 20 wt%, an increase of Ti atoms is detected on the hybrid films surface. However, the concentration of Ti atoms on the hybrid films surface levels off as the TiO_2 content more than 20 wt%. Moreover, the shifts of titanium signals in XPS spectra are correlated with titanium atoms in different chemical states.

5.9 References

1. R. C. Mehrota, R. Bohra, D. P. Gaur, *Metal β-Diketonates and Allied Derivatives, Academic London* (1978).
2. M. Guglielmi, G. Carturan, *J. Non-Cryst. Solids* 100: 16 (1988).
3. H. Schmidt, B. Seiferling, *Mater. Res. Soc. Symp. Proc.* 73: 739 (1986).
4. H. L. Tyan, Y. C. Liu, K. H. Wei, *Polymer* 40: 4877 (1999).
5. L. Liu, Q. Lu, J. Yin, X. Qian, W. Wang, Z. Zhu, Z. Wang, *Mater. Chem. Phys.* 74: 210 (2002).
6. Q. Hu, E. Marand, *Polymer* 40: 4833 (1999).
7. L. H. Lee, W. C. Chen, *Chem. Mater.* 13: 1137 (2001).
8. J. Zhang, B. J. Wang, X. Ju, T. Liu, T. D. Hu, *Polymer* 42: 3697 (2001).
9. C. Sanchez, J. Livage, M. Henry, F. Babonneau, *J. of Non-Cryst. Solid* 100: 65 (1988).
10. M. Yoshida, M. Lal, N. D. Kumar, P. N. Prasad, *J. of Mat. Sci.* 32: 4047 (1997).
11. D. P. Heberer, S. Z. D. Cheng, J. S. Barley, S. H. S. Lien, R. G. Bryant, F. W. Harris, *Macromolecules* 24(8): 1890 (1991).
12. M. E. Rogers, M. H. Brink, J. E. Mcgrath, A. Brennan, *Polymer* 34(4): 849 (1993).
13. C. Koning, L. Teuwen, E. W. Meijer, J. Moonen, *Polymer* 35(22): 4889 (1994).
14. X. Q. Liu, K. Yamanaka, M. Jikei, *Chem. Mater.* 12(12): 3885 (2000).
15. S. Tamai, T. Kuroki, A. Shibuya, *Polymer* 42(6): 2373 (2001).
16. M. R. Benjaram, C. Biswajit, *Langmuir* 17: 1132 (2001).
17. E. Bedri, A. H. Robert, W. S. Gary, S. David, L. D. Victoria, S. Mohamed, *Langmuir* 17: 2664 (2001).
18. G. Christophe, D. Evelyne, D. Philippe, D. Michel, *Journal of Electron Spectroscopy and Related Phenomena* 70: 11 (1994).

19. G. M. Porta, J. D. Rancourt, L. T. Taylor, *Chem. Mater.* 1: 269 (1989).

20. M. Nandi, J. A. Conklin, L. Salvati, A. Sen, *Chem. Mater.* 3: 201 (1991).

21. R. K. Boggess, L. T. Taylor, *J. Polym. Sci., Polym. Chem.* 25: 685 (1987).

22. J. D. Rancourt, L. T. Taylor, *Macromolecules* 20: 790 (1987).